ELSEVIER

Journal of Crystal Growth 234 (2002) 399–403

JOURNAL OF CRYSTAL GROWTH

www.elsevier.com/locate/jcrysgro

Observation of carbon clusters of a few nanometers in the oxyacetylene diamond CVD process

Hyo-S. Ahn[a], Hyun-M. Park[b], Doh-Y. Kim[a], Nong M. Hwang[a,b,*]

[a] *Center for Microstructure Science of Materials, School of Materials Science & Engineering, Seoul National University, Building 37, Room 106, Seoul 151-742, South Korea*

[b] *Korea Research Institute of Standards and Science, P.O. Box 102, Daejon 305-600, South Korea*

Received 19 June 2001; accepted 25 September 2001

Communicated by D.T.J. Hurle

Abstract

We observed the carbon clusters by TEM after capturing them on a grid membrane during the oxyacetylene flame diamond synthesis. The clusters of ~ 1.5 nm captured on the amorphous membrane in the gas mixture of the acetylene-to-oxygen ratio of 1.04 were mostly amorphous with a few having a diamond lattice. The clusters larger than 5 nm captured at the gas ratio of 1.09 were mostly graphite with a minor fraction of diamond.

PACS: 36.40.W; 81.05.T; 68.55.J; 52.75.R

Keywords: A1. Nanostructure; A1. Nucleation; A3. Chemical vapor deposition processes; B1. Diamond

---

In spite of intensive studies on the CVD diamond growth [1–5], the growth mechanism is not yet clearly understood. Among the suggested mechanisms, one thing is common; the atomic hydrogen is essential to the CVD diamond growth although its exact role is not generally agreed upon. A drastically different growth mechanism, the charged cluster model (CCM), was suggested by Hwang et al. [6–8]. In the CCM, it was predicted that the charged carbon clusters of a few nanometers should be generated in the CVD diamond reactor and suspended like colloidal particles in the gas phase with their subsequent deposition as diamond films. In the CVD diamond process, the CCM can explain some unusual phenomena taking place in the CVD diamond process, which were difficult to approach by the conventional concept of atomic growth. For example, the CCM can avoid the thermodynamic paradox in explaining the well-known phenomenon of simultaneous diamond deposition and graphite etching. Besides, the CCM can explain satisfactorily the preferential formation of diamond particles on the apex over the valley of the substrate. The relatively easy formation of diamond on the graphite surface in the new diamond CVD process can also be successfully explained by

---

*Corresponding author. Center for Microstructure Science of Materials, School of Materials Science & Engineering, Seoul National University, Building 37, Room 106, Seoul 151-742, South Korea. Tel.: +82-2-880-8922; fax: +82-2-882-8164.

E-mail address: nmhwang@kriss.re.kr (N.M. Hwang).

PII: S0022-0248(01)01748-1

the CCM. The CCM also explains the evolution of porous skeletal soot on some transition metals such as Fe, Ni and Co and of diamond films on other substrates such as Si, W and Mo under the identical processing condition.

Recently, these hypothetical charged carbon clusters were experimentally confirmed by an energy analyzer and a Wien filter in the hot filament diamond CVD process [9,10]. As predicted in the CCM [8], the cluster size increased with increasing methane concentration [10]. Under the condition when the clusters of a few hundreds of atoms were generated, the good quality diamond crystals were deposited while under the condition when the clusters of more than one thousand atoms were generated, the cauliflower-shaped or ball-like diamonds were deposited. If these diamond clusters continue to grow in the gas phase, they can grow into the diamond particles in the size range between nanometers to micrometers. Indeed, these diamond particles were confirmed earlier in other groups in the gas phase of the low-pressure diamond synthesis by microwave plasma [11], DC plasma jet [12] and laser [13,14].

Since diamond films can be synthesized by the oxyacetylene flame [15], the carbon clusters are also expected to form in the gas phase. Indeed, the existence of charged carbon clusters in the flame of a gas mixture of hydrocarbon and oxygen was confirmed by Homann group using an energy analyzer [16], a Wien filter [17] and a time-of-flight (TOF) [18] in their study of combustion and flame. Although they did not relate the generation of charged carbon clusters to the CVD diamond growth, the ratio of carbon to oxygen they used ranged from 1.0 to 1.2, which is close to the composition for diamond CVD using the oxyacetylene flame [15]. In their measurements, the cluster size increased with increasing ratio of carbon to oxygen. They reported that the carbon clusters containing hundreds to thousands of atoms were either positively or negatively charged. By TOF analyses [18], they further showed that the positively charged clusters were hydrogenated, which are known as polyaromatic hydrocarbon (PAH) ions, while the negatively charged ones were almost of pure carbon. The purpose of this paper is to capture these clusters on a membrane during the oxyacetylene flame diamond CVD process and to observe them by TEM with the similar procedure used in the TEM observation of Si [19], ZrO_2 [20] and Au [21] clusters.

In order to capture the carbon clusters during the oxyacetylene diamond CVD process, a Mo mesh grid coated with an amorphous silica membrane for TEM was used. The copper mesh grid was inappropriate for this experiment because copper tended to evaporate during the exposure in the oxyacetylene flame and the copper clusters, which have a similar structure to diamond, landed on the membrane. A commercial oxyacetylene torch with a nozzle of 1 mm diameter was used. Two different ratios of acetylene to oxygen of 1.04 and 1.09 were used to compare the cluster size. The exposure time of the TEM grid in the flame was 10, 30 and 60 s for the gas ratio of 1.04 and 10 s for the ratio of 1.09. When the exposure time is longer than 10 s for the gas ratio of 1.09, the deposits were too thick for TEM observation.

The total flow rate of acetylene and oxygen was 2 l/min. The acetylene flame consists of three parts: inner flame, outer flame and acetylene feather. The length of the total flame depended on the gas ratio and the flow rate. With the flow rate of 2 liter per min, the flame length was 20 and 25 mm for the gas ratios of 1.04 and 1.09, respectively.

In a preliminary experiment to decide the position of the grid in the flame, the films were deposited with varying distances between the nozzle and the silicon substrate. The substrate was placed on the water-cooled copper plate. Diamond crystals were deposited in the flame 16 mm away from the nozzle for the gas ratio of 1.04. Graphitic films were deposited in the flame 12.5 mm away from the nozzle for the gas ratio of 1.09. Therefore, the Mo grids were placed at 16 and 12.5 mm away from the nozzle for the gas ratios of 1.04 and 1.09, respectively. The surface temperature of the water-cooled copper plate was measured to be 600°C by the thermocouple buried in the copper plate. The actual grid temperature was estimated to be 700–800°C or even higher, considering that the silica membrane tended to melt with the prolonged exposure in the flame.

Figs. 1(a)–(c) show carbon clusters captured for 10, 30 and 60 s, respectively, with the gas ratio of

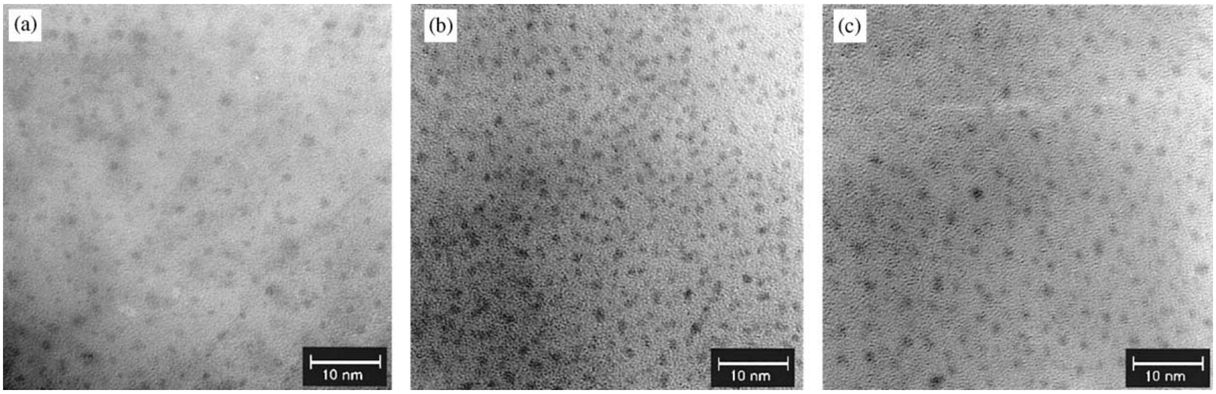

Fig. 1. TEM microstructures of carbon clusters captured on the silica membrane for (a) 10 s, (b) 30 s and (c) 60 s with a gas ratio of $C_2H_2:O_2 = 1.04$ during the flame deposition of diamond.

1.04 in the oxyacetylene flame. Individual clusters are shown as dark spots. Isolated clusters with an average size of 1.5 nm are distributed uniformly on an amorphous silica membrane. The number density of clusters was $2.1 \times 10^{11}/\text{mm}^2$ after 10 s, increased to $3.2 \times 10^{11}/\text{mm}^2$ after 30 s but decreased to $2.0 \times 10^{11}/\text{mm}^2$ after 60 s. The decrease in the number density between 30 and 60 s was repeatedly reproduced. This means that the clusters are being etched away after some initial period under the identical processing conditions.

The similar phenomenon of simultaneous cluster deposition and atomic etching occurs in the diamond CVD using the C–H system [7] and in the silicon CVD using the Si–Cl–H system [22,23]. In these systems, the gas phase solubility of carbon or silicon increases with decreasing temperature near the substrate temperature and the gas phase nucleation changes the driving force at the substrate temperature from deposition to etching. Unlike the C–H system, the gas phase nucleation does not change the driving force for etching on the substrate in the C–H–O system using the gas ratio of acetylene to oxygen of 1.04 [24,25]. However, the oxyacetylene torch CVD process is done in an open air and the outer flame must be oxygen rich due to the supply of oxygen from the air. This excess oxygen coming from the air appears to make the driving force for etching on the substrate.

In the initial stage before 30 s, the cluster flux landing on the membrane must have exceeded the atomic flux of etching, which results in the increase of the number density of carbon clusters with deposition time. As the charged clusters continue to land on the insulating membrane, the electric charge will build up. This built-up charge will exert the Coulomb repulsion on the incoming charged clusters especially when they have the same sign of the charge. Thus, the cluster flux landing on the membrane will decrease with processing time. If the flux for atomic etching exceeds the flux for cluster landing, the number density of clusters on the membrane will decrease. This picture explains the decrease in the number density of clusters after 60 s in Fig. 1(c). Most of clusters shown in Fig. 1 appear to etch away during prolonged deposition, judging from the final diamond grain size of a few microns evolved after prolonged deposition.

Although most clusters in Fig. 1 were amorphous, a few of them have a lattice fringe as shown in Fig. 2, which is a high-resolution image of Fig. 1(c). Lattice spacing was 2.06 Å, which indicates the spacing of {1 1 1} plane of diamond. The amorphous clusters in Fig. 1 are not necessarily amorphous in the gas phase. The structure of clusters, especially small ones, is greatly influenced by the surface they land on. The small clusters have a strong tendency for structural accommodation with the surface on which they land [26]. Even if the clusters have the diamond structure in the

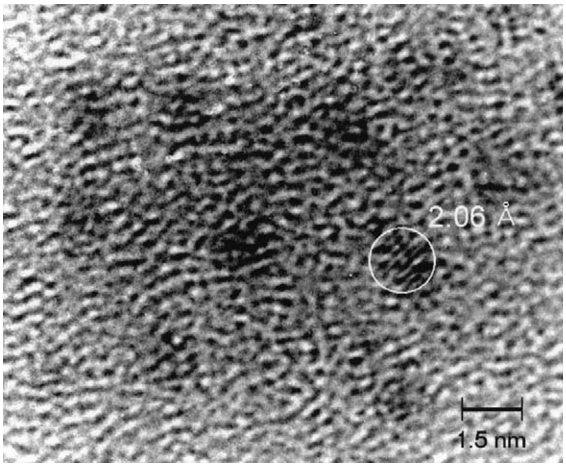

Fig. 2. High resolution TEM image of the cluster with the diamond lattice, observed among the clusters in Fig. 1(c).

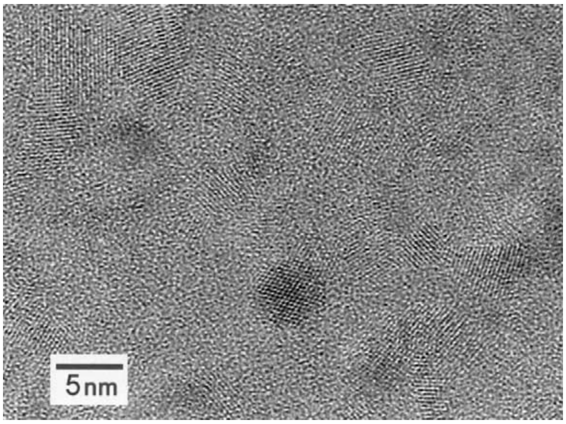

Fig. 3. High resolution TEM image of the clusters captured for 10 s with a gas ratio of C_2H_2:O_2 = 1.09.

gas phase, they might change to the amorphous structure on the amorphous membrane. This possibility was revealed in the study of gold clusters captured on the amorphous silica membrane [21]. Small clusters (2.4 nm) were amorphous while large ones (8 nm) had a gold lattice.

Fig. 3 shows the high resolution TEM image of the carbon clusters captured for 10 s at 12.5 mm away from the nozzle for the gas ratio of 1.09. Compared with the clusters in Fig. 1, the clusters in Fig. 3 are much larger (> 5 nm) and have a lattice fringe. Most clusters have a graphite lattice and only a minor fraction of them has a diamond lattice. The high resolution TEM image of Fig. 3 reveals a lattice fringe spacing of 0.312 nm, which can be matched with the electron diffraction pattern shown in Fig. 4. The ring pattern of Fig. 4 could be indexed with the graphite phase (JCPDS 25-0284, $P6_3/mmc$, $a = 0.2456$ nm, $c = 0.6696$ nm) [27] although there is a slight difference in the low-index diffraction. For example, the spacing of the (0 0 2) planes is contracted by 0.0228 nm (6.8%) compared with that of the JCPDS data. This contraction might come from the high capillary pressure of the graphite cluster of ~5 nm.

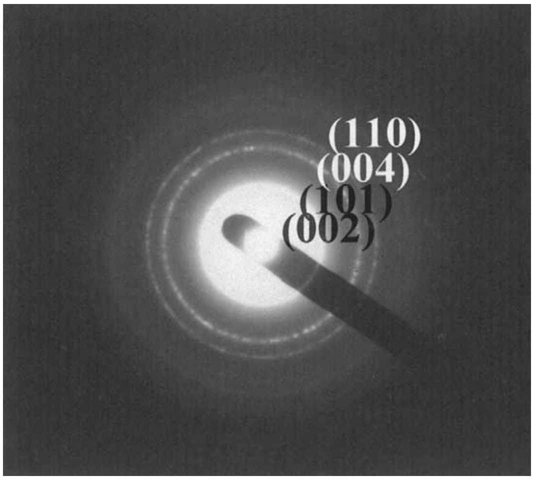

Fig. 4. Typical electron diffraction pattern of the sample for Fig. 3, showing the polycrystalline graphite.

As shown previously by molecular dynamics simulation of gold clusters [26], the small clusters, if landing on the growing gold surface, undergo epitaxial recrystallization instantly while the large clusters tend to make twin or grain boundaries. Since the diamond films are grown under the processing condition to produce the clusters in Fig. 1, the small clusters in Fig. 1 are expected to undergo homoepitaxial recrystallization after landing on the diamond surface. However, the large graphite clusters in Fig. 3 would have difficulty in epitaxial recrystallization on the growing surface and make frequent secondary nucleation, leading to a graphite nanostructure.

The clusters in Fig. 3 have mostly a graphite lattice instead of a diamond one, indicating that graphite is more stable than diamond for these clusters. This result is in contrast with the diamond lattice of the small cluster shown in Fig. 2. There are two possibilities for stabilization of graphite over diamond for the clusters in Fig. 3. One is the size effect on the stability between diamond and graphite [6]. In order for diamond to be stable over graphite by the capillary effect, the clusters may have to be smaller than those in Fig. 3. In other words, the clusters in Fig. 3 may be large enough for graphite to be stable over diamond. The other possibility is that the clusters are electrically neutralized after positively and negatively charged clusters coagulate together. Thus, the stability of the charged diamond clusters achieved by the electrical double layer [28] is lost after charge neutralization. Although in the hot filament diamond CVD process, clusters are dominantly negatively charged, both positively and negatively charged clusters are formed in abundance in the flame of the oxyhydrocarbon gas mixture [16]. Further studies should be done to clarify this stability problem.

Conclusively, the carbon clusters of a few nanometers were observed by TEM after being captured on a grid membrane in the oxyacetylene flame diamond CVD process. The clusters of 1.5 nm, which were produced in the acetylene-to-oxygen ratio of 1.04, were mostly amorphous on the amorphous silica membrane. The clusters larger than 5 nm, which were produced in the gas ratio of 1.09, were mostly graphite with a minor fraction of diamond.

Acknowledgements

This work was supported by the Creative Research Initiatives Program of Korea Ministry of Science and Technology. TEM observations by Mr. Hyun Ryu at Korea Research Institute of Standards and Science are greatly appreciated.

References

[1] B.V. Spitsyn, L.L. Bouilov, B.V. Derjaguin, J. Crystal Growth 52 (1981) 219.
[2] S. Matsumoto, Y. Sato, M. Tsutumi, N. Setaka, J. Mater. Sci. 17 (1982) 3106.
[3] J.C. Angus, C.C. Hayman, Science 241 (1988) 913.
[4] J.E. Butler, F.G. Celii, P.E. Pehrsson, H.-T. Wang, H.H. Nelson, Mater. Res. Soc. Symp. Proc. 131 (1989) 259.
[5] W.A. Yarbrough, J. Am. Ceram. Soc. 75 (1992) 3179.
[6] N.M. Hwang, J.H. Hahn, D.Y. Yoon, J. Crystal Growth 160 (1996) 87.
[7] N.M. Hwang, D.Y. Yoon, J. Crystal Growth 160 (1996) 98.
[8] N.M. Hwang, J.H. Hahn, D.Y. Yoon, J. Crystal Growth 162 (1996) 55.
[9] I.D. Jeon, C.J. Park, D.Y. Kim, N.M. Hwang, J. Crystal Growth 213 (2000) 79.
[10] I.D. Jeon, C.J. Park, D.Y. Kim, N.M. Hwang, J. Crystal Growth 223 (2001) 6.
[11] M. Frenklach, R. Kematick, D. Huang, W. Howard, K.E. Spear, J. Appl. Phys. 66 (1989) 395.
[12] Z. Chang, X. Jiang, S. Qin, X. Zhang, Z. Xue, S. Pang, Gas phase nucleation of diamond in plasma jet, Second International Conference on Applications of Diamond Films and Related Materials, Tokyo, Japan, 1993, p. 463.
[13] P.R. Buerki, S. Leutwyler, J. Appl. Phys. 69 (1991) 3739.
[14] P.R. Buerki, S. Leutwyler, J. Nanostruct. Mater. 4 (1994) 577.
[15] P.K. Bachmann, D. Leers, H. Lydtin, Diamond Relat. Mater. 1 (1991) 1.
[16] P. Gerhardt, K.H. Homann, Combust. Flame 81 (1990) 289.
[17] K.H. Homann, J. Traube, Ber. Bunsenges. Phys. Chem. 91 (1987) 828.
[18] P. Gerhardt, K.H. Homann, J. Phys. Chem. 94 (1990) 5381.
[19] W.S. Cheong, N.M. Hwang, D.Y. Yoon, J. Crystal Growth 204 (1999) 52.
[20] I.D. Jeon, L. Gueroudji, D.Y. Kim, N.M. Hwang, J. Korean Ceram. Soc. 38 (2001) 218.
[21] M.C. Barnes, D.Y. Kim, H.S. Ahn, C.O. Lee, N.M. Hwang, J. Crystal Growth 213 (2000) 83.
[22] N.M. Hwang, J. Crystal Growth 205 (1999) 59.
[23] N.M. Hwang, W.S. Cheong, D.Y. Yoon, J. Crystal Growth 206 (1999) 177.
[24] N.M. Hwang, J. Crystal Growth 135 (1994) 165.
[25] L. Gueroudji, N.M. Hwang, Diamond Relat. Mater. 9 (2000) 205.
[26] S.-C. Lee, N.M. Hwang, B.D. Yu, D.-Y. Kim, J. Crystal Growth 223 (2001) 311.
[27] JCDPS 25-0284, Holcomb, USAEC Oak Ridge Y-12 Plant, Report Y 1887, 1973.
[28] N.M. Hwang, D.Y. Kim, J. Crystal Growth 218 (2000) 40.